

1 **ONLINE SUPPORTING INFORMATION**

2 **Contents**

3 Derivation of limiting case predictions for synchrony of per capita growth rates  
4 (Equations 3-4) . . . . . 4  
5 Materials and methods details . . . . . 8  
6 Vital rate statistical models . . . . . 8  
7 Multi-species populations models . . . . . 9  
8 Results for synchrony of percent cover . . . . . 11  
9 Supporting Figures . . . . . 12  
10 Supporting Tables . . . . . 18  
11 Interaction Coefficients for Vital Rates in Arizona . . . . . 19  
12 Interaction Coefficients for Vital Rates in Idaho . . . . . 20  
13 Interaction Coefficients for Vital Rates in Kansas . . . . . 21  
14 Interaction Coefficients for Vital Rates in Montana . . . . . 22  
15 Interaction Coefficients for Vital Rates in New Mexico . . . . . 23  
16 References . . . . . 24

17 **List of Figures**

18 S1 Observed (vertical dashed lines) and simulated (solid density curves) synchrony  
19 of species per capita growth rates at each site from the IBM (top panels) and the  
20 IPM (bottom panels). IPM density curves come from 100 random contiguous  
21 sections from 2,000 iteration IPM runs, where the length of each randomly  
22 selected section is equal to the number of observation years for each data set.  
23 IBM density curves come from 100 replicate simulations of 75 iterations each.  
24 Synchrony values come from simulations where environmental stochasticity  
25 and interspecific interactions are present. The IBM was run on a 5 by 5 meter  
26 landscape to reduce the effect of demographic stochasticity. . . . . 12

|    |    |  |    |
|----|----|--|----|
| 27 | S2 | Community-wide synchrony of species percent cover from model simulation experiments. Synchrony of species' percent cover for each study area are from simulation experiments with demographic stochasticity, environmental stochasticity, and interspecific competition present ("All Drivers"), demographic stochasticity removed ("No D.S."), environmental stochasticity removed ("No E.S."), interspecific competition removed ("No Comp."), interspecific competition and demographic stochasticity removed ("No Comp. + No D.S."), and interspecific competition and environmental stochasticity removed ("No Comp. + No E.S."). Abbreviations within the bars for the New Mexico site indicate whether the IBM or IPM was used for a particular simulation. Error bars represent the 2.5% and 97.5% quantiles from model simulations. . . . . | 13 |
| 38 | S3 | Synchrony of species' percent cover for each study area from IBM simulations across different landscape sizes when only demographic stochasticity is present ("D.S. Only") and when environmental stochasticity is also present removed ("D.S. + E.S."). The horizontal lines show the analytical predictions $\mathcal{M}_D$ (dashed line) and $\mathcal{M}_E$ (dotted line). The strength of demographic stochasticity decreases as landscape size increases because population sizes also increase. Error bars represent the 2.5% and 97.5% quantiles from model simulations. .   | 14 |
| 45 | S4 | Variance of percent cover for each species (along x-axes) in each site through time from simulations with only environmental stochasticity operating (IPM with no species interactions). . . . .   | 15 |
| 48 | S5 | Variance of per capita growth rates for each species (along x-axes) in each site through time from simulations with only environmental stochasticity operating (IPM with no species interactions). . . . .   | 15 |
| 51 | S6 | Variance of percent cover for each species (along x-axes) in each site through time from simulations with only demographic stochasticity operating (IBM simulated on 5 by 5 meter landscape). . . . .  | 16 |
| 54 | S7 | Variance of per capita growth rates for each species (along x-axes) in each site through time from simulations with only demographic stochasticity operating (IBM simulated on 5 by 5 meter landscape). . . . .  | 16 |
| 57 | S8 | Community-wide synchrony of species' growth rates from model simulation experiments for the Idaho community with <i>Artemisia tripartita</i> removed. Synchrony of species' growth rates are from simulation experiments with demographic stochasticity, environmental stochasticity, and interspecific competition present ("All Drivers"), demographic stochasticity removed ("No D.S."), environmental stochasticity removed ("No E.S."), interspecific competition removed ("No Comp."), interspecific competition and demographic stochasticity removed ("No Comp. + No D.S."), and interspecific competition and environmental stochasticity removed ("No Comp. + No E.S."). Error bars represent the 2.5% and 97.5% quantiles from model simulations. . . . .   | 17 |

## 67 List of Tables

|    |     |   |    |
|----|-----|---|----|
| 68 | S1  | Comparisons between our analytical predictions and simulation results for synchrony of species' per capita growth rates. Analytical predictions represent two limiting cases where only demographic stochasticity is operating ( $\phi_{R, \mathcal{M}_D}$ ) and where only environmental stochasticity is operating ( $\phi_{R, \mathcal{M}_E}$ ). Simulated synchrony values come from our empirically-based, multi-species population models when simulated under conditions that match the limiting case conditions (e.g., environmental stochasticity and competition removed for $\mathcal{M}_D$ ). . . . . | 18 |
| 69 |     |   |    |
| 70 |     |   |    |
| 71 |     |   |    |
| 72 |     |   |    |
| 73 |     |   |    |
| 74 |     |   |    |
| 75 | S2  | Percent differences of synchrony of per capita growth rates between each removal simulation experiment and the 'All Drivers' simulation. . . . .  | 18 |
| 76 |     |   |    |
| 77 | S3  | Correlations of species' year random effects for each site by term, where term refers to the random effect on the slope or the intercept. . . . .   | 19 |
| 78 |     |   |    |
| 79 | S4  | Average interaction coefficients for each vital rate for each community. . . . .  | 19 |
| 80 | S5  | Interaction coefficients for growth regressions in Arizona. . . . .   | 19 |
| 81 | S6  | Interaction coefficients for survival regressions in Arizona. . . . .   | 20 |
| 82 | S7  | Interaction coefficients for recruitment regressions in Arizona. . . . .  | 20 |
| 83 | S8  | Interaction coefficients for growth regressions in Idaho. . . . .   | 20 |
| 84 | S9  | Interaction coefficients for survival regressions in Idaho. . . . .   | 21 |
| 85 | S10 | Interaction coefficients for recruitment regressions in Idaho. . . . .  | 21 |
| 86 | S11 | Interaction coefficients for growth regressions in Kansas. . . . .  | 21 |
| 87 | S12 | Interaction coefficients for survival regressions in Kansas. . . . .  | 22 |
| 88 | S13 | Interaction coefficients for recruitment regressions in Kansas. . . . .   | 22 |
| 89 | S14 | Interaction coefficients for growth regressions in Montana. . . . .   | 22 |
| 90 | S15 | Interaction coefficients for survival regressions in Montana. . . . .   | 23 |
| 91 | S16 | Interaction coefficients for recruitment regressions in Montana. . . . .  | 23 |
| 92 | S17 | Interaction coefficients for growth regressions in NewMexico. . . . .   | 23 |
| 93 | S18 | Interaction coefficients for survival regressions in NewMexico. . . . .   | 24 |
| 94 | S19 | Interaction coefficients for recruitment regressions in NewMexico. . . . .  | 24 |

95 **Derivation of limiting case predictions for synchrony of per capita**  
 96 **growth rates (Equations 3-4)**

97 Following Loreau and de Mazancourt (2013) and de Mazancourt et al. (2013), we define  
 98 population growth, ignoring observation error, as

$$r_i(t) = r_{mi} \left[ 1 - \frac{N_i(t) + \sum_{j \neq i} \alpha_{ij} N_j(t)}{K_i} + \sigma_{ei} u_{ei}(t) + \frac{\sigma_{di} u_{di}(t)}{\sqrt{N_i(t)}} \right] \quad (\text{S1})$$

99 where  $N_i(t)$  is the biomass of species  $i$  in year  $t$ , and  $r_i(t)$  is its growth rate in year  $t$ .  $r_{mi}$  is  
 100 species  $i$ 's intrinsic rate of increase,  $K_i$  is its carrying capacity, and  $\alpha_{ij}$  is the interspecific  
 101 competition coefficient representing the effect of species  $j$  on species  $i$ . Environmental  
 102 stochasticity is incorporated as  $\sigma_{ei} u_{ei}(t)$ , where  $\sigma_{ei}^2$  is the environmental variance and  $u_{ei}$  are  
 103 normal random variables with zero mean and unit variance that are independent through  
 104 time but may be correlated between species. Demographic stochasticity arises from variations  
 105 in births and deaths among individuals (e.g., same states, different fates), and is included in  
 106 the model as a first order, normal approximation (Lande et al. 2003, de Mazancourt et al.  
 107 2013).  $\sigma_{di}^2$  is the demographic variance and  $u_{di}(t)$  are independent normal variables with zero  
 108 mean and unit variance.

109 First-order approximations of the temporal variance of total community biomass are obtained  
 110 as follows (Ives 1995, Hughes and Roughgarden 2000, Ives and Hughes 2002, Loreau and de  
 111 Mazancourt 2008, de Mazancourt et al. 2013). Let  $\delta N_i(t) = N_i(t) - N_i^*$  denote the deviation  
 112 of observed species  $i$ 's biomass from its equilibrium value in the community,  $N_i^*$ , in the  
 113 absence of stochasticity. Equation (S1) can be Taylor expanded around  $\delta N_i(t) = u_{ei}(t) =$   
 114  $u_{di}(t) = u_{oi}^S(t) = 0$  to yield, after dropping terms of order two and higher,

$$\delta \mathbf{N}(t+1) = \mathbf{A} \delta \mathbf{N}(t) + \mathbf{z}(t), \quad (\text{S2})$$

115 where  $\delta \mathbf{N}(t)$  is the vector of deviations of species biomasses from their deterministic equi-  
 116 librium value,  $\mathbf{A}$  is the community matrix, also known as the Jacobian matrix around the  
 117 equilibrium, with elements  $(a_{ij})_{1 < i, j < S}$ :

$$A_{ij} = \begin{cases} 1 - r_{mi} \frac{N_i^*}{K_i}, & i = j \\ -r_{mi} \frac{N_i^*}{K_i} \alpha_{ij}, & i \neq j \end{cases} \quad (\text{S3})$$

118 and  $\mathbf{z}(t)$  is a vector that encapsulates the effects of environmental and demographic stochas-  
 119 ticity whose elements are

$$z_i(t) = N_i^* \sigma_{ei} u_{ei}(t) + \sqrt{N_i^*} \sigma_{di} u_{di}(t) \quad (\text{S4})$$

120 When the system reaches a stationary distribution, the variances and covariances between  
 121 species biomass time series are:

$$\langle \delta \mathbf{N}(t) \delta \mathbf{N}(t)^T \rangle = \mathbf{C}^\infty = (\text{cov}(N_i, N_j))_{1 < i, j < S} = (\text{cov}(\delta N_i, \delta N_j))_{1 < i, j < S} \quad (\text{S5})$$

122 where  $\delta \mathbf{N}^T$  is the transpose of vector  $\delta \mathbf{N}$ , i.e. a row vector.

123 Our assumptions listed above lead to the following correlation structure of  $\mathbf{z}$ :

$$\langle \mathbf{z}(t) \mathbf{z}(t)^T \rangle = \mathbf{B} \quad (\text{S6})$$

$$\langle \mathbf{z}(t-s) \mathbf{z}(t)^T \rangle = 0 \quad \text{for } s > 0 \quad (\text{S7})$$

124 We use Equation S2 to write a dynamical equation for the covariance  $\mathbf{C}$ :

$$\mathbf{C}(t+1) = \langle \delta \mathbf{N}(t+1) \delta \mathbf{N}(t+1)^T \rangle \quad (\text{S8})$$

$$= \mathbf{A} \langle \delta \mathbf{N}(t) \delta \mathbf{N}(t)^T \rangle \mathbf{A}^T + \mathbf{A} \langle \delta \mathbf{N}(t) \delta \mathbf{N}(t)^T \rangle + \langle \mathbf{z}(t) \delta \mathbf{N}(t)^T \rangle \mathbf{A}^T + \langle \mathbf{z}(t) \mathbf{z}(t)^T \rangle \quad (\text{S9})$$

$$= \mathbf{A} \mathbf{C}(t) \mathbf{A}^T + \mathbf{Z}_0 \quad (\text{S10})$$

125

126 Taking the limit  $t \rightarrow \infty$  on both sides, we get:

$$\mathbf{C}^\infty = \mathbf{A} \mathbf{C}^\infty \mathbf{A}^T + \mathbf{B} \quad (\text{S11})$$

127 where  $\mathbf{A}$  is as in Equation S3 and  $\mathbf{B}$  is:

$$B_{ij} = N_i^* N_j^* \sigma_{ei} \sigma_{ej} \text{cov}(u_{ei}, u_{ej}) + \sqrt{N_i^* N_j^*} \sigma_{di} \sigma_{dj} \text{cov}(u_{di}, u_{dj}) \quad (\text{S12})$$

128 Similarly,  $\mathbf{R}$  is the variance-covariance matrix for population growth rates at steady state

$$R_{ij} = \frac{r_{mi} r_{mj}}{K_i K_j} \sum_{k,l} \alpha_{ik} \alpha_{jl} C_{kl} + \sigma_{ei} \sigma_{ej} \text{cov}(u_{ei}, u_{ej}) + \frac{\sigma_{di} \sigma_{dj} \text{cov}(u_{di}, u_{dj})}{\sqrt{N_i^* N_j^*}}. \quad (\text{S13})$$

129 Then, following the synchrony metric of Loreau and de Mazancourt (2008), the synchrony of  
 130 population biomasses is

$$\phi_N = \frac{\sum_{i,j} C_{ij}}{\left( \sum_i \sqrt{C_{ii}} \right)^2} \quad (\text{S14})$$

131 and the synchrony of per capita growth rates is

$$\phi_R = \frac{\sum_{i,j} R_{ij}}{\left(\sum_i \sqrt{R_{ii}}\right)^2}. \quad (\text{S15})$$

132 Synchrony of population biomasses and growth rates emerge from complex interactions among  
 133 species' intrinsic growth rates, interspecific interactions, environmental stochasticity, and  
 134 demographic stochasticity. Given these complexities, it is impossible to determine expected  
 135 effects of different parameters in a multi-species case. Thus, we analyze a simplified case where  
 136 interspecific interactions are zero. The variance-covariance matrix of population biomasses at  
 137 steady state then becomes

$$c_{ij} = \frac{B_{ij}}{1 - A_i A_j} = \frac{N_i^* N_j^* \sigma_{ei} \sigma_{ej} \text{COV}(u_{ei}, u_{ej}) + \sqrt{N_i^* N_j^*} \sigma_{di} \sigma_{dj} \text{COV}(u_{di}, u_{dj})}{1 - (1 - r_{mi})(1 - r_{mj})} \quad (\text{S16})$$

138 and the variance-covariance matrix of population growth rates simplifies to

$$R_{ij} = \frac{1}{1 - \frac{r_{mi} r_{mj}}{r_{mi} + r_{mj}}} \left( \sigma_{ei} \sigma_{ej} \text{COV}(u_{ei}, u_{ej}) + \frac{\sigma_{di} \sigma_{dj} \text{COV}(u_{di}, u_{dj})}{\sqrt{N_i^* N_j^*}} \right) \quad (\text{S17})$$

139 Note that synchrony in population sizes and synchrony in growth rates use weighted factors  
 140 of the environmental variances and covariances with species-specific parameters. So, we  
 141 further assume that, along with interspecific interactions being zero, all species have identical  
 142 growth rates, environmental stochasticity is absent, and all species have identical demographic  
 143 variance. This represents a theoretical limiting case where the community consists of identical  
 144 species coexisting in a constant environment where only demographic stochasticity causes  
 145 temporal fluctuations. Under such conditions, synchrony of population biomasses is

$$\phi_N = \frac{1}{\left(\sum_i p_i^{1/2}\right)^2} \quad (\text{S18})$$

146 and synchrony of growth rates is

$$\phi_R = \frac{\sum_i p_i^{-1}}{\left(\sum_i p_i^{-1/2}\right)^2} \quad (\text{S19})$$

147 where  $p_i$  is the average frequency of species  $i$ ,  $p_i = N_i/N_T$ . When all species have identical  
 148 abundances and  $p_i = 1/S$ , where  $S$  is species richness, the both synchrony values equal  $1/S$   
 149 (Loreau and de Mazancourt 2008). The prediction represented in Equation S19 is Equation 3  
 150 in the main text, which we refer to as  $\phi_{R, \mathcal{M}_D}$ .

151 Another limiting case is where only environmental stochasticity is operating: no interspecific  
 152 interactions, no demographic stochasticity, identical intrinsic growth rates, and environmental  
 153 stochasticity with same standard deviation for all species. Under such constraints, the  
 154 synchrony of of species' biomasses is

$$\phi_N = \sum_{i,j} p_i p_j \text{cov}(u_{ei}, u_{ej}) \quad (\text{S20})$$

155 and the synchrony of species' growth rates is

$$\phi_R = \frac{\sum_{i,j} \text{cov}(u_{ei}, u_{ej})}{S^2} \quad (\text{S21})$$

156 The prediction represented in Equation S21 is Equation 4 in the main text, which we refer  
 157 to as  $\phi_{R, \mathcal{M}_E}$ . If we know the covariance matrix of the species environmental responses, we  
 158 can calculate the above expectations directly. Note that the environmental responses are  
 159 normalized in the above equations, therefore the covariances are correlations in the above  
 160 equations.

161 **Materials and methods details**

162 **Vital rate statistical models**

163 We modeled survival probability and growth on individual genets as a function of genet size,  
 164 the crowding experienced by the focal genet from both heterospecific and conspecific genets  
 165 in its neighborhood (described below), temporal variation among years, and spatial variation  
 166 among quadrat groups. Groups are sets of quadrats located in close proximity within a  
 167 pasture or grazing enclosure.

168 We follow the approach of Chu and Adler (2015) to estimate crowding, assuming that the  
 169 crowding experienced by a focal genet depends on distance to each neighbor genet and the  
 170 neighbor's size,  $u$ :

$$w_{ijm,t} = \sum_k e^{-\delta_{jm} d_{ijkm,t}^2} u_{km,t}. \quad (\text{S22})$$

171 In the above,  $w_{ijm,t}$  is the crowding that genet  $i$  of species  $j$  in year  $t$  experiences from  
 172 neighbors of species  $m$ . The spatial scale over which species  $m$  neighbors exert influence  
 173 on any genet of species  $j$  is determined by  $\delta_{jm}$ . The function is applied for all  $k$  genets of  
 174 species  $m$  that neighbor the focal genet at time  $t$ , and  $d_{ijkm,t}$  is the distance between genet  $i$   
 175 in species  $j$  and genet  $k$  in species  $m$ . When  $k = m$ , the effect is intraspecific crowding. We  
 176 use regression-specific (survival and growth)  $\delta$  values estimated by Chu and Adler (2015).

177 We used logistic regression to model survival probability ( $S$ ) of genet  $i$  from species  $j$  in  
 178 quadrat group  $g$  from time  $t$  to  $t + 1$ :

$$\text{logit}(S_{ijg,t}) = \gamma_{j,t}^S + \phi_{jg}^S + \beta_{j,t}^S x_{ij,t} + \boldsymbol{\omega}_j^S \mathbf{w}_{ij,t} \quad (\text{S23})$$

179 where  $x_{ij,t}$  is the log of genet size,  $\gamma_{j,t}^S$  is a year-specific intercept,  $\beta_{j,t}^S$  is the year-specific slope  
 180 parameter for size,  $\phi_{jg}^S$  is the random effect of quadrat group location, and  $\boldsymbol{\omega}$  is a vector of  
 181 per capita interaction coefficients which determine the impact of crowding,  $\mathbf{w}$ , by each species  
 182 on the focal species.

183 We modeled genet growth, conditional on survival, in a similar manner:

$$\mu_{ijg,t+1} = \gamma_{j,t}^G + \phi_{jg}^G + \beta_{j,t}^G \mu_{ij,t} + \boldsymbol{\omega}_j^G \mathbf{w}_{ij,t} \quad (\text{S24})$$

184 where  $\mu$  is log genet size and all other parameters are as described for the survival regression.  
 185 We capture non-constant error variance in growth by modeling the variance around the  
 186 growth regression ( $\varepsilon$ ) as a nonlinear function of predicted genet size:

$$\varepsilon_{ij,t} = ae^{b\mu_{ijg,t+1}} \quad (\text{S25})$$



187 Our data allows us to track new recruits, but we cannot assign a specific parent to new genets.  
 188 Therefore, we model recruitment at the quadrat level: the number of new individuals of  
 189 species  $j$  in quadrat  $q$  recruiting at time  $t + 1$  as a function of quadrat “effective cover” ( $A'$ ) in  
 190 the previous year ( $t$ ). Effective cover is a mixture of observed cover ( $A$ ) in the focal quadrat  
 191 ( $q$ ) and the mean cover across the entire group ( $\bar{A}$ ) of  $Q$  quadrats in which  $q$  is located:

$$A'_{jq,t} = p_j A_{jq,t} + (1 - p_j) \bar{A}_{jQ,t} \quad (\text{S26})$$

192 where  $p$  is a mixing fraction between 0 and 1 that is estimated within the model.

193 We assume the number of individuals,  $y^R$ , recruiting at time  $t + 1$  follows a negative binomial  
 194 distribution:

$$y^R_{jq,t+1} \sim \text{NegBin}(\lambda_{jq,t+1}, \zeta) \quad (\text{S27})$$

195 where  $\lambda$  is the mean intensity and  $\zeta$  is the size parameter. We define  $\lambda$  as:

$$\lambda_{jq,t+1} = A'_{jq,t} e^{(\gamma^R_{j,t} + \phi^R_{jQ} + \theta^R_{jk} C_{k,t} + \omega^R \sqrt{A'_{q,t}})} \quad (\text{S28})$$

196 where  $A'$  is effective cover ( $\text{cm}^2$ ) of species  $j$  in quadrat  $q$  and all other terms are as in the  
 197 survival and growth regressions.

## 198 Multi-species populations models

199 The individually based model (IBM) is straightforward and described in the main text, so here  
 200 focus on the structure of the integral projection model (IPM). We built an environmentally  
 201 stochastic IPM. Our IPM follows the specification of Chu and Adler (2015) where the  
 202 population of species  $j$  is a density function  $n(u_j, t)$  giving the density of sized- $u$  genets at  
 203 time  $t$ . Genet size is on the natural log scale, so that  $n(u_j, t) du$  is the number of genets whose  
 204 area (on the arithmetic scale) is between  $e^{u_j}$  and  $e^{u_j+du}$ . So, the density function for any size  
 205  $v$  at time  $t + 1$  is

$$n(v_j, t + 1) = \int_{L_j}^{U_j} k_j(v_j, u_j, \bar{\mathbf{w}}_j(u_j)) n(u_j, t) \quad (\text{S29})$$

206 where  $k_j(v_j, u_j, \bar{\mathbf{w}}_j)$  is the population kernel that describes all possible transitions from size  $u$   
 207 to  $v$  and  $\bar{\mathbf{w}}_j$  is a vector of estimates of average crowding experienced from all other species  
 208 by a genet of size  $u_j$  and species  $j$ . The integral is evaluated over all possible sizes between  
 209 predefined lower ( $L$ ) and upper ( $U$ ) size limits that extend beyond the range of observed  
 210 genet sizes.

211 The population kernel is defined as the joint contributions of survival ( $S$ ), growth ( $G$ ), and  
 212 recruitment ( $R$ ):

$$k_j(v_j, u_j, \bar{\mathbf{w}}_j) = S_j(u_j, \bar{\mathbf{w}}_j(u_j)) G_j(v_j, u_j, \bar{\mathbf{w}}_j(u_j)) + R_j(v_j, u_j, \bar{\mathbf{w}}_j), \quad (\text{S30})$$

213 which means we are calculating growth ( $G$ ) for individuals that survive ( $S$ ) from time  $t$  to  
214  $t+1$  and adding in newly recruited ( $R$ ) individuals of an average sized one-year-old genet for  
215 the focal species. Our stastical model for recruitment ( $R$ , described below) returns the number  
216 of new recruit produced per quadrat. Following previous work, we assume that fecundity  
217 increases linearly with size ( $R_j(v_j, u_j, \bar{\mathbf{w}}_j) = e^{u_j} R_j(v_j, \bar{\mathbf{w}}_j)$ ) to incorporate the recruitment  
218 function in the spatially-implicit IPM.

## 219 Results for synchrony of percent cover

220 Synchrony of percent cover from population model simulations did not compare well with  
221 observed synchrony of cover or analytical predictions for synchrony cover (Fig. S2, S3). We  
222 did not expect synchrony of percent cover from simulations to compare well with observed  
223 synchrony of cover because our models represent equilibrium dynamics rather than a specific  
224 set of observed years. Also, unlike growth rates, synchrony in cover is highly influenced by  
225 drift and legacy effects (Loreau and de Mazancourt 2008).

226 More interesting is that our simulation results did not compare well with analytical predictions.  
227 One issue is that some species are not well-regulated around their equilibrium cover, so  
228 that our linear approximation required for analytical predictions is likely to fail. Analytical  
229 predictions for synchrony of growth rates are more informative than synchrony in population  
230 sizes because the linear approximation is more proximate.

231 Another issue is the influence of demographic stochasticity in some communities, for example,  
232 in Idaho where our simulations with only demographic stochasticity yielded results far  
233 different from analytical predictions (Fig. S2). Our analytical predictions require the  
234 unrealistic assumption that demographic variances among species are equal. However, in  
235 Idaho, *A. tripartita* has much higher demographic stochasticity than the other species, so  
236 that variation in its abundance dominates. Thus, the assumption that all species have similar  
237 stochasticity fails. In combination, our results from analyzing synchrony of percent cover  
238 indicate that the best way to decipher the mechanisms contributing to community synchrony  
239 is to analyze growth rates, in agreement with the theoretical arguments of Loreau and de  
240 Mazancourt (2008).

241 **Supporting Figures**

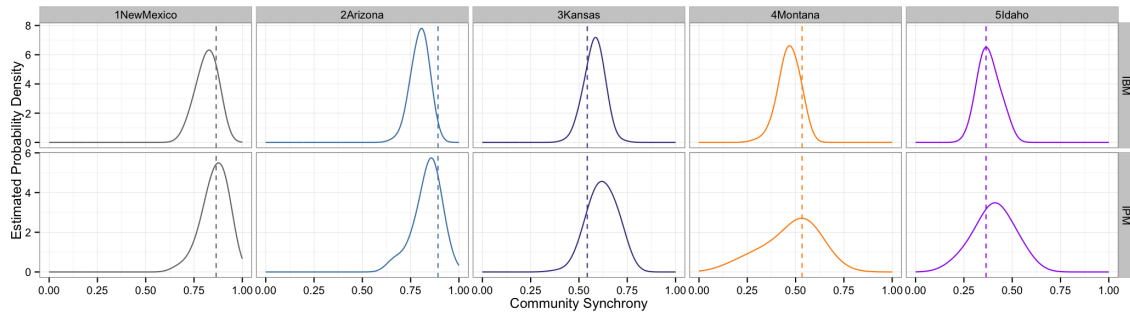


Figure S1: Observed (vertical dashed lines) and simulated (solid density curves) synchrony of species per capita growth rates at each site from the IBM (top panels) and the IPM (bottom panels). IPM density curves come from 100 random contiguous sections from 2,000 iteration IPM runs, where the length of each randomly selected section is equal to the number of observation years for each data set. IBM density curves come from 100 replicate simulations of 75 iterations each. Synchrony values come from simulations where environmental stochasticity and interspecific interactions are present. The IBM was run on a 5 by 5 meter landscape to reduce the effect of demographic stochasticity.

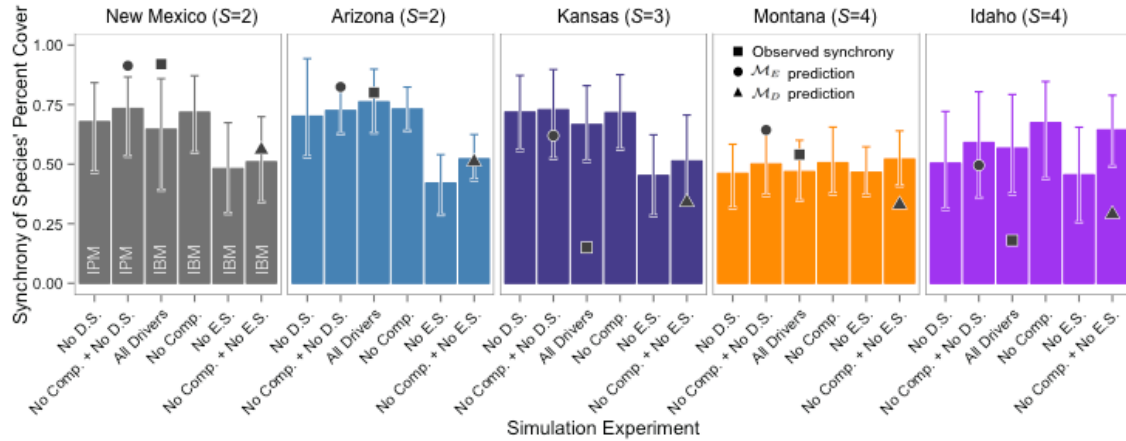


Figure S2: Community-wide synchrony of species percent cover from model simulation experiments. Synchrony of species' percent cover for each study area are from simulation experiments with demographic stochasticity, environmental stochasticity, and interspecific competition present (“All Drivers”), demographic stochasticity removed (“No D.S.”), environmental stochasticity removed (“No E.S.”), interspecific competition removed (“No Comp.”), interspecific competition and demographic stochasticity removed (“No Comp. + No D.S.”), and interspecific competition and environmental stochasticity removed (“No Comp. + No E.S.”). Abbreviations within the bars for the New Mexico site indicate whether the IBM or IPM was used for a particular simulation. Error bars represent the 2.5% and 97.5% quantiles from model simulations.

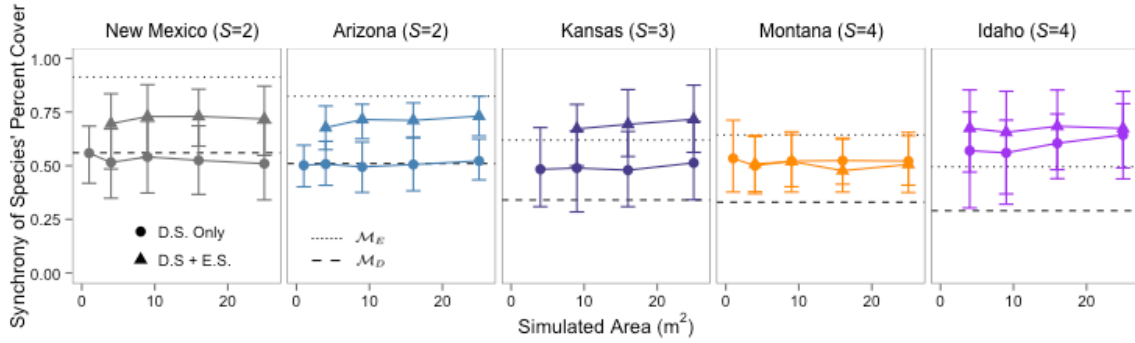


Figure S3: Synchrony of species' percent cover for each study area from IBM simulations across different landscape sizes when only demographic stochasticity is present (“D.S. Only”) and when environmental stochasticity is also present removed (“D.S. + E.S.”). The horizontal lines show the analytical predictions  $\mathcal{M}_D$  (dashed line) and  $\mathcal{M}_E$  (dotted line). The strength of demographic stochasticity decreases as landscape size increases because population sizes also increase. Error bars represent the 2.5% and 97.5% quantiles from model simulations.

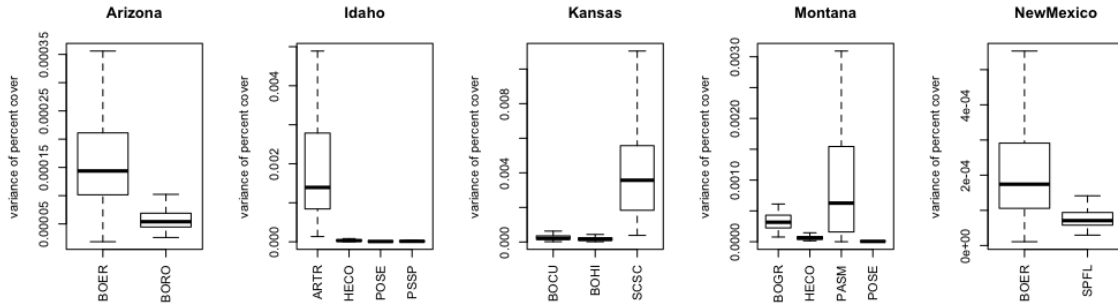


Figure S4: Variance of percent cover for each species (along x-axes) in each site through time from simulations with only environmental stochasticity operating (IPM with no species interactions).

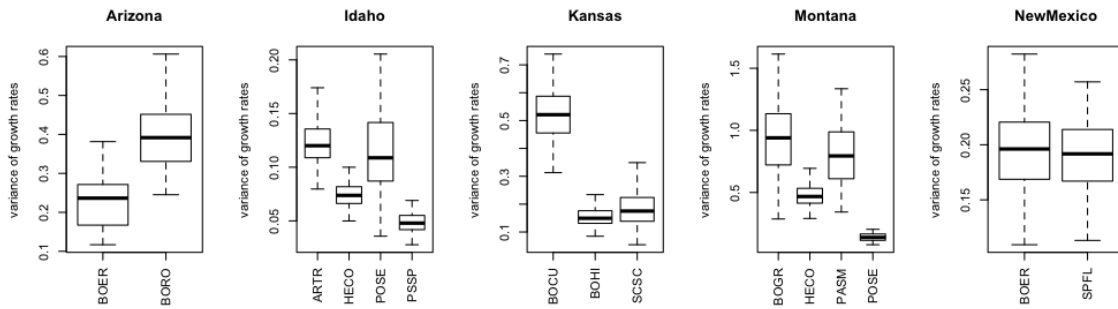


Figure S5: Variance of per capita growth rates for each species (along x-axes) in each site through time from simulations with only environmental stochasticity operating (IPM with no species interactions).

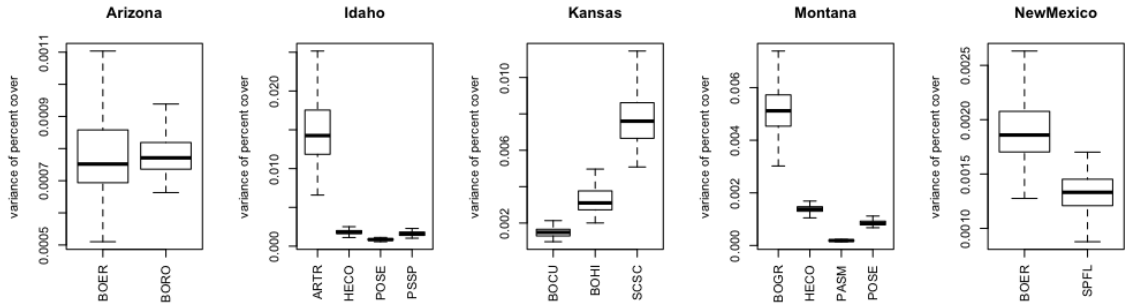


Figure S6: Variance of percent cover for each species (along x-axes) in each site through time from simulations with only demographic stochasticity operating (IBM simulated on 5 by 5 meter landscape).

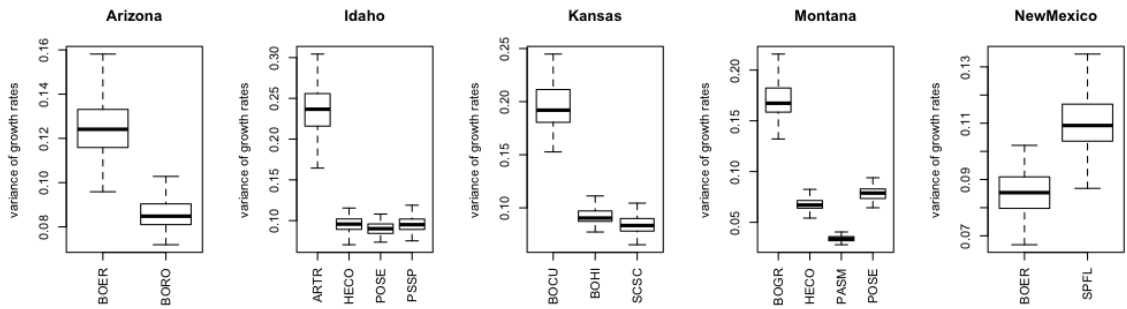


Figure S7: Variance of per capita growth rates for each species (along x-axes) in each site through time from simulations with only demographic stochasticity operating (IBM simulated on 5 by 5 meter landscape).



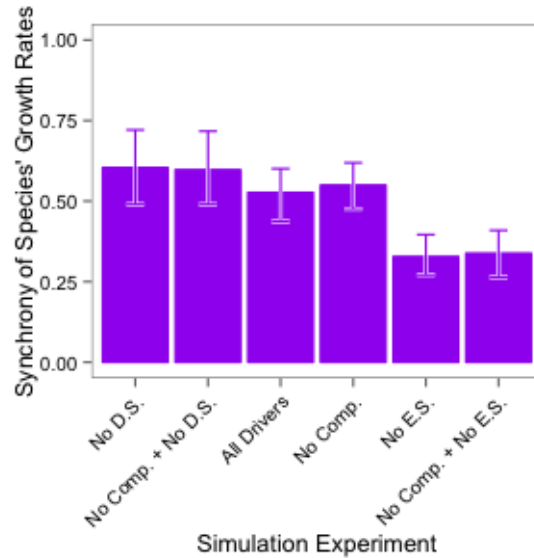


Figure S8: Community-wide synchrony of species' growth rates from model simulation experiments for the Idaho community with *Artemisia tripartita* removed. Synchrony of species' growth rates are from simulation experiments with demographic stochasticity, environmental stochasticity, and interspecific competition present ("All Drivers"), demographic stochasticity removed ("No D.S."), environmental stochasticity removed ("No E.S."), interspecific competition removed ("No Comp."), interspecific competition and demographic stochasticity removed ("No Comp. + No D.S."), and interspecific competition and environmental stochasticity removed ("No Comp. + No E.S."). Error bars represent the 2.5% and 97.5% quantiles from model simulations.

## 242 Supporting Tables

243 In all tables, species codes are as follows (also see Table 1 in the main text):

- 244 • *Bouteloua eriopoda* = BOER
- 245 • *Sporobolus flexuosus* = SPFL
- 246 • *Bouteloua rothrockii* = BORO
- 247 • *Bouteloua curtipendula* = BOCU
- 248 • *Bouteloua hirsuta* = BOHI
- 249 • *Schizachyrium scoparium* = SCSC
- 250 • *Bouteloua gracilis* = BOGR
- 251 • *Hesperostipa comata* = HECO
- 252 • *Pascopyrum smithii* = PASM
- 253 • *Poa secunda* = POSE
- 254 • *Artemisia tripartita* = ARTR
- 255 • *Pseudoroegneria spicata* = PSSP

Table S1: Comparisons between our analytical predictions and simulation results for synchrony of species' per capita growth rates. Analytical predictions represent two limiting cases where only demographic stochasticity is operating ( $\phi_{R,\mathcal{M}_D}$ ) and where only environmental stochasticity is operating ( $\phi_{R,\mathcal{M}_E}$ ). Simulated synchrony values come from our empirically-based, multi-species population models when simulated under conditions that match the limiting case conditions (e.g., environmental stochasticity and competition removed for  $\mathcal{M}_D$ ).

| Site       | Predicted $\phi_{R,\mathcal{M}_D}$ | Simulated $\phi_{R,\mathcal{M}_D}$ | Predicted $\phi_{R,\mathcal{M}_E}$ | Simulated $\phi_{R,\mathcal{M}_E}$ |
|------------|------------------------------------|------------------------------------|------------------------------------|------------------------------------|
| New Mexico | 0.56                               | 0.51                               | 0.86                               | 0.86                               |
| Arizona    | 0.51                               | 0.52                               | 0.82                               | 0.81                               |
| Kansas     | 0.35                               | 0.39                               | 0.62                               | 0.62                               |
| Montana    | 0.31                               | 0.31                               | 0.47                               | 0.50                               |
| Idaho      | 0.29                               | 0.31                               | 0.43                               | 0.42                               |

Table S2: Percent differences of synchrony of per capita growth rates between each removal simulation experiment and the 'All Drivers' simulation.

| simulation          | 1New Mexico | 2Arizona | 3Kansas | 4Montana | 5Idaho |
|---------------------|-------------|----------|---------|----------|--------|
| 1No D.S.            | 5.53        | 4.28     | 6.01    | 5.27     | 11.95  |
| 2No Comp. + No D.S. | 5.56        | 2.06     | 7.03    | 6.21     | 9.10   |
| 4No Comp.           | 0.98        | 0.06     | 4.84    | 1.43     | 0.11   |
| 5No E.S.            | 40.14       | 33.20    | 47.84   | 39.06    | 9.28   |
| 6No Comp. + No E.S. | 45.95       | 41.48    | 38.21   | 39.44    | 20.33  |

Table S3: Correlations of species' year random effects for each site by term, where term refers to the random effect on the slope or the intercept.

| site      | term      | growth | recruit | surv |
|-----------|-----------|--------|---------|------|
| Arizona   | intercept | 0.51   | -0.05   | 0.51 |
| Arizona   | slope     | 0.68   |         | 0.16 |
| Idaho     | intercept | 0.45   | 0.38    | 0.25 |
| Idaho     | slope     | 0.50   |         | 0.47 |
| Kansas    | intercept | 0.44   | 0.29    | 0.26 |
| Kansas    | slope     | 0.19   |         | 0.16 |
| Montana   | intercept | 0.29   | 0.07    | 0.41 |
| Montana   | slope     | 0.11   |         | 0.02 |
| NewMexico | intercept | 0.51   | -0.15   | 0.65 |
| NewMexico | slope     | 0.37   |         | 0.20 |

Table S4: Average interaction coefficients for each vital rate for each community.

| Site      | Interaction Type | Growth  | Recruitment | Survival |
|-----------|------------------|---------|-------------|----------|
| Arizona   | Interspecific    | -0.0111 | -0.4534     | -0.0507  |
| Arizona   | Intraspecific    | -0.0402 | -1.4209     | -0.4446  |
| Idaho     | Interspecific    | 0.0022  | -0.1091     | 0.0059   |
| Idaho     | Intraspecific    | -0.0469 | -1.5569     | -0.5269  |
| Kansas    | Interspecific    | -0.0008 | 0.0463      | -0.0041  |
| Kansas    | Intraspecific    | -0.0062 | -0.9945     | -0.0586  |
| Montana   | Interspecific    | -0.0059 | 0.0691      | 0.0342   |
| Montana   | Intraspecific    | -0.0801 | -2.0900     | -0.8652  |
| NewMexico | Interspecific    | -0.0027 | -0.3461     | -0.0080  |
| NewMexico | Intraspecific    | -0.0111 | -1.6473     | -0.2191  |

Table S5: Interaction coefficients for growth regressions in Arizona.

|      | BOER    | BORO    |
|------|---------|---------|
| BOER | -0.0033 | -0.0171 |
| BORO | -0.0050 | -0.0772 |

Table S6: Interaction coefficients for survival regressions in Arizona.

|      | BOER    | BORO    |
|------|---------|---------|
| BOER | -0.2791 | -0.0814 |
| BORO | -0.0200 | -0.6102 |

Table S7: Interaction coefficients for recruitment regressions in Arizona.

|      | BOER    | BORO    |
|------|---------|---------|
| BOER | -0.5184 | -0.3290 |
| BORO | -0.5779 | -2.3235 |

Table S8: Interaction coefficients for growth regressions in Idaho.

|      | ARTR    | HECO    | POSE    | PSSP    |
|------|---------|---------|---------|---------|
| ARTR | -0.0300 | 0.0129  | 0.0117  | 0.0003  |
| HECO | -0.0000 | -0.0285 | 0.0084  | -0.0028 |
| POSE | 0.0001  | 0.0032  | -0.0845 | -0.0043 |
| PSSP | -0.0003 | -0.0027 | -0.0004 | -0.0448 |

Table S9: Interaction coefficients for survival regressions in Idaho.

|      | ARTR    | HECO    | POSE    | PSSP    |
|------|---------|---------|---------|---------|
| ARTR | -0.0236 | -0.0199 | 0.0314  | 0.0158  |
| HECO | -0.0005 | -1.0206 | -0.0051 | 0.0125  |
| POSE | 0.0001  | 0.0006  | -0.9088 | 0.0121  |
| PSSP | 0.0009  | -0.0013 | 0.0248  | -0.1547 |

Table S10: Interaction coefficients for recruitment regressions in Idaho.

|      | ARTR    | HECO    | POSE    | PSSP    |
|------|---------|---------|---------|---------|
| ARTR | -0.4003 | 0.2243  | 0.0117  | 0.2360  |
| HECO | -0.5681 | -1.7594 | -0.1437 | -0.3195 |
| POSE | -0.2505 | -0.0131 | -2.2928 | -0.1420 |
| PSSP | -0.2405 | -0.1389 | 0.0347  | -1.7751 |



Table S11: Interaction coefficients for growth regressions in Kansas.

|      | BOCU    | BOHI    | SCSC    |
|------|---------|---------|---------|
| BOCU | -0.0017 | 0.0011  | 0.0010  |
| BOHI | 0.0002  | -0.0046 | -0.0078 |
| SCSC | -0.0003 | 0.0007  | -0.0124 |

Table S12: Interaction coefficients for survival regressions in Kansas.

|      | BOCU    | BOHI    | SCSC    |
|------|---------|---------|---------|
| BOCU | -0.1084 | 0.0006  | 0.0010  |
| BOHI | 0.0021  | -0.0403 | -0.0153 |
| SCSC | -0.0064 | -0.0066 | -0.0271 |

Table S13: Interaction coefficients for recruitment regressions in Kansas.

|      | BOCU    | BOHI    | SCSC    |
|------|---------|---------|---------|
| BOCU | -1.1544 | -0.0312 | -0.0643 |
| BOHI | 0.3410  | -0.8681 | 0.0041  |
| SCSC | 0.0619  | -0.0336 | -0.9611 |

Table S14: Interaction coefficients for growth regressions in Montana.

|      | BOGR    | HECO    | PASM    | POSE    |
|------|---------|---------|---------|---------|
| BOGR | -0.0124 | -0.0032 | -0.0258 | -0.0001 |
| HECO | -0.0025 | -0.0976 | 0.0096  | 0.0079  |
| PASM | -0.0006 | -0.0041 | -0.0695 | -0.0030 |
| POSE | 0.0006  | -0.0082 | -0.0417 | -0.1410 |

Table S15: Interaction coefficients for survival regressions in Montana.

|      | BOGR    | HECO    | PASM    | POSE    |
|------|---------|---------|---------|---------|
| BOGR | -0.1316 | 0.0076  | 0.1096  | 0.0126  |
| HECO | -0.0028 | -0.7064 | 0.1423  | -0.0030 |
| PASM | -0.0012 | -0.0033 | -1.4026 | 0.0024  |
| POSE | 0.0014  | 0.0082  | 0.1363  | -1.2203 |

Table S16: Interaction coefficients for recruitment regressions in Montana.

|      | BOGR    | HECO    | PASM    | POSE    |
|------|---------|---------|---------|---------|
| BOGR | -0.9151 | -0.3076 | -0.0984 | 0.0495  |
| HECO | -0.0785 | -1.4192 | -0.0480 | -0.0468 |
| PASM | -0.0103 | 0.2773  | -4.3148 | 0.3470  |
| POSE | 0.1971  | 0.4854  | 0.0623  | -1.7109 |

Table S17: Interaction coefficients for growth regressions in NewMexico.

|      | BOER    | SPFL    |
|------|---------|---------|
| BOER | -0.0045 | -0.0013 |
| SPFL | -0.0041 | -0.0176 |

Table S18: Interaction coefficients for survival regressions in NewMexico.

|      | BOER    | SPFL    |
|------|---------|---------|
| BOER | -0.1576 | -0.0040 |
| SPFL | -0.0120 | -0.2806 |

Table S19: Interaction coefficients for recruitment regressions in NewMexico.

|      | BOER    | SPFL    |
|------|---------|---------|
| BOER | -0.7649 | -0.6230 |
| SPFL | -0.0691 | -2.5296 |

## 261 **References**

- 262 Chu, C., and P. B. Adler. 2015. Large niche differences emerge at the recruitment stage to  
263 stabilize grassland coexistence. *Ecological Monographs* 85:373–392.
- 264 de Mazancourt, C., F. Isbell, A. Larocque, F. Berendse, E. De Luca, J. B. Grace, B. Haegeman,  
265 H. Wayne Polley, C. Roscher, B. Schmid, D. Tilman, J. van Ruijven, A. Weigelt, B. J. Wilsey,  
266 and M. Loreau. 2013. Predicting ecosystem stability from community composition and  
267 biodiversity. *Ecology Letters* 16:617–625.
- 268 Hughes, J. B., and J. Roughgarden. 2000. Species Diversity and Biomass Stability. *The*  
269 *American Naturalist* 155:618–627.
- 270 Ives, A. 1995. Predicting the Response of Populations to Environmental Change. *Ecology*  
271 76:926–941.
- 272 Ives, A. R., and J. B. Hughes. 2002. General Relationships Between Species Diversity and  
273 Stability in Competitive Systems. *The American Naturalist* 159:388–395.
- 274 Lande, R., S. Engen, and B.-E. Saether. 2003. Stochastic population dynamics in ecology  
275 and conservation.
- 276 Loreau, M., and C. de Mazancourt. 2008. Species synchrony and its drivers: neutral and  
277 nonneutral community dynamics in fluctuating environments. *The American Naturalist*  
278 172:E48–E66.
- 279 Loreau, M., and C. de Mazancourt. 2013. Biodiversity and ecosystem stability: A synthesis  
280 of underlying mechanisms. *Ecology Letters* 16:106–115.